Supplementary Materials for

Astrocyte reactivity impairs lymphopoiesis through cholesterol-dependent mTOR suppression in common lymphoid progenitors

Rui Zhao *et al.*

⁎Corresponding author. Fang Ni, fangni@ustc.edu.cn

This Word file includes:

Supplementary Fig. S1 to S9 and Figure Legends

Table S1. Clinical characteristics of samples from patients with neuroimmune disorders

Supplementary Fig. S1

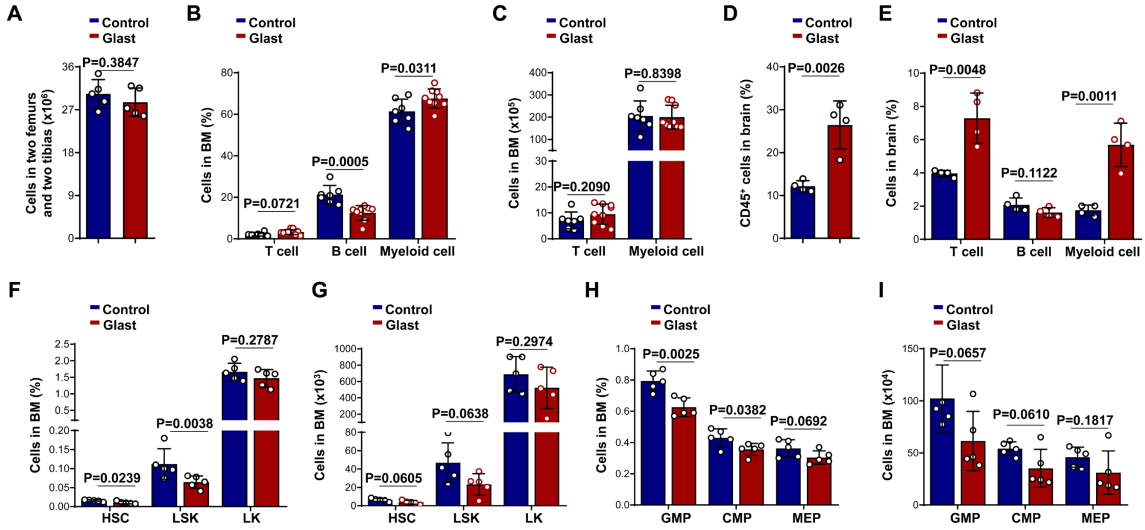

Supplementary Fig. S1: Slc1a3/Glast-lineage CNS perturbation selectively affects lymphoid cells while largely preserving myeloid and HSPC compartments.

A, Total bone marrow (BM) cell counts from two femurs and two tibias of Glast-CreERT;DTA and control mice (*n* = 5 per group). **B-C,** Flow cytometric analysis of the frequencies **(B)** and absolute numbers **(C)** of T cells (CD3⁺), B cells (B220⁺), and myeloid cells (CD11b⁺Gr-1⁺) in the BM (*n* = 7-9 per group). **D**, CD45⁺ leukocyte frequencies in whole-brain homogenates from Glast-CreERT;DTA and control mice (*n* = 4 per group). **E,** Frequencies of T cells (CD3⁺), B cells (B220⁺), and myeloid cells (CD11b⁺Gr-1⁺) among CD45⁺ brain-infiltrating leukocytes (*n* = 4 per group). **F, G**, Frequencies **(F)** and absolute numbers **(G)** of HSCs, LSK cells, and LK cells in BM (*n* = 5 per group). **H-I,** Frequencies **(H)** and absolute numbers **(I)** of granulocyte-monocyte progenitors (GMPs), common myeloid progenitors (CMPs), and megakaryocyte-erythroid progenitors (MEPs) in the BM (*n* = 5 per group). Data are presented as mean ± s.d. *P* values were determined by two-tailed unpaired Student's *t*-tests between Glast-CreERT;DTA and control groups. All experiments were independently repeated at least twice.

Supplementary Fig. S2

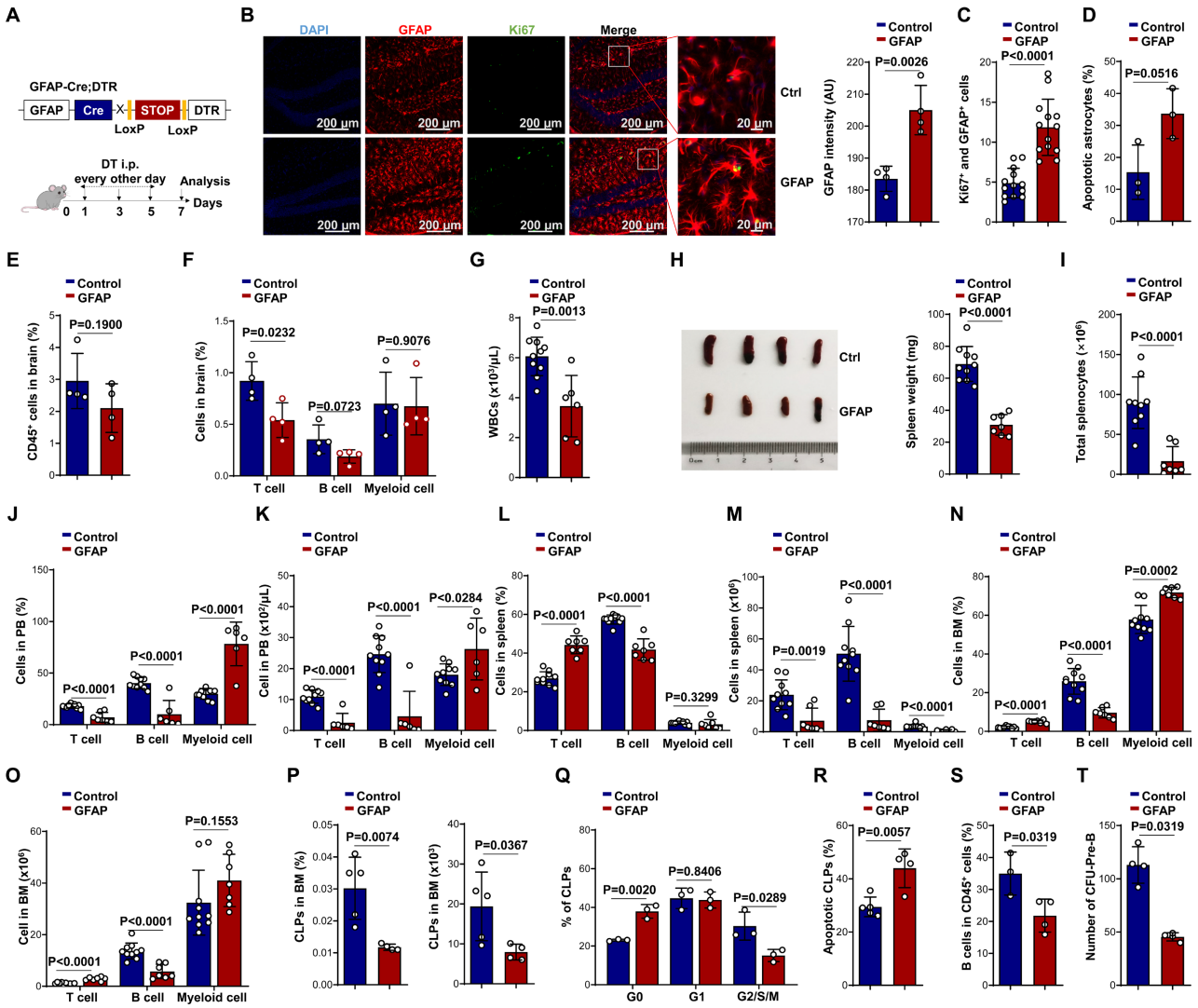

Supplementary Fig. S2: GFAP-lineage perturbation is associated with reactive gliosis and impaired lymphoid differentiation.

A, Schematic and experimental timeline for the GFAP-Cre;DTR model. Diphtheria toxin (DT, 5 μg/kg) was administered intraperitoneally on days 1, 3, and 5; analysis was performed on day 7. **B,** Representative immunofluorescence images of hippocampal sections showing GFAP⁺ astrocytes (red) and Ki-67⁺ proliferating cells (green). Nuclei were stained with DAPI (blue). Insets show higher magnification views. Scale bars: 200 μm (overview) and 20 μm (insets) ($n = 4$ per group). **C,** Quantification of GFAP⁺ and Ki-67⁺ cells in the hippocampus ($n = 13$ per group). **D,** Astrocyte apoptosis as assessed by flow cytometry for Annexin V⁺ cells in DT-treated primary astrocyte cultures ($n = 3$ mice per group). **E,** CD45⁺ leukocyte frequencies in whole-brain

homogenates ($n = 4$ mice per group). **F,** Composition of brain-infiltrating leukocytes: $CD3^+$ T cells, $B220^+$ B cells, and $CD11b^+Gr\text{-}1^+$ myeloid cells ($n = 4$ mice per group). **G-I,** White blood cell (WBC) counts in peripheral blood **(G)**, spleen morphology (**H**, representative images and spleen weight), and total splenocyte counts **(I)** ($n = 7$ for GFAP-Cre;DTR, $n = 10$ for controls). **J-O,** Frequencies **(J, L, N)** and absolute numbers **(K, M, O)** of $CD3^+$ T cells, $B220^+$ B cells, and $CD11b^+Gr\text{-}1^+$ myeloid cells in peripheral blood **(J, K)**, spleen **(L, M)**, and bone marrow (BM) **(N, O)** ($n = 6$-7 for GFAP-Cre;DTR, $n = 10$ for controls). **P,** CLP frequencies (left) and absolute numbers (right) in the BM ($n = 4$ for GFAP-Cre;DTR, $n = 5$ for controls). **Q,** Cell-cycle analysis of BM CLPs ($n = 3$ mice per group). **R,** Apoptosis of BM CLPs as assessed by Annexin V staining ($n = 4$ mice per group). **S,** *In vitro* B-cell differentiation was evaluated by co-culturing sorted Lin^- BM cells (5×10^4) with OP9 stroma for 12 days, followed by flow cytometric analysis of $B220^+$ B-cell differentiation ($n = 3$-4 mice per group). **T**, Pre-B cell colony-formation potential was assessed by culturing BM cells in methylcellulose under lymphoid-promoting conditions ($n = 4$ mice per group). Data are presented as mean ± s.d. *P*-values were determined by two-tailed unpaired Student's *t*-tests between GFAP-Cre;DTR and control groups. All experiments were independently replicated at least twice.

Supplementary Fig. S3

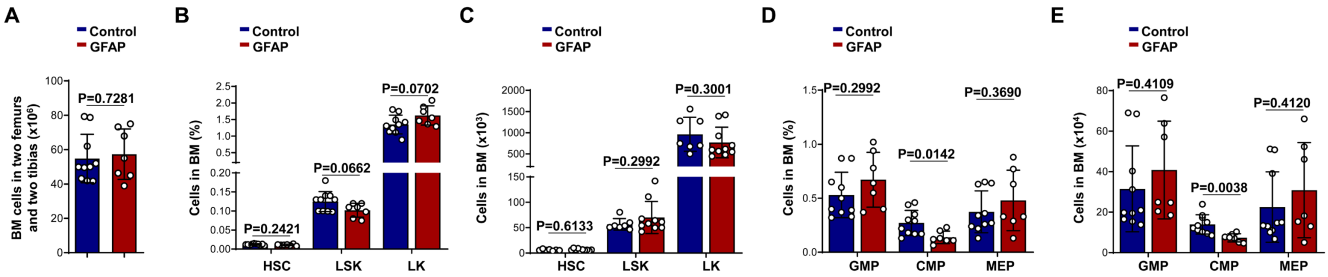

Supplementary Fig. S3: GFAP-lineage perturbation does not substantially alter HSPC and myeloid progenitor composition in bone marrow.

A, Total bone marrow (BM) cellularity from two femurs and two tibias in GFAP-Cre;DTR and control mice ($n = 7$ for GFAP-Cre;DTR, $n = 10$ for controls). **B-C,** Frequencies **(B)** and absolute numbers **(C)** of HSPCs, including HSCs, LSK cells, and LK cells in BM measured by flow cytometry ($n = 7$ for GFAP-Cre;DTR, $n = 10$ for controls). **D-E,** Frequencies **(D)** and absolute numbers **(E)** of granulocyte-monocyte progenitors (GMPs), common myeloid progenitors (CMPs), and megakaryocyte-erythroid progenitors (MEPs) in BM ($n = 7$ for GFAP-Cre;DTR, $n = 10$ for controls). Data are presented as mean ± s.d. *P* values were calculated using two-tailed unpaired Student's *t*-tests. All experiments were independently replicated at least twice.

Supplementary Fig. S4

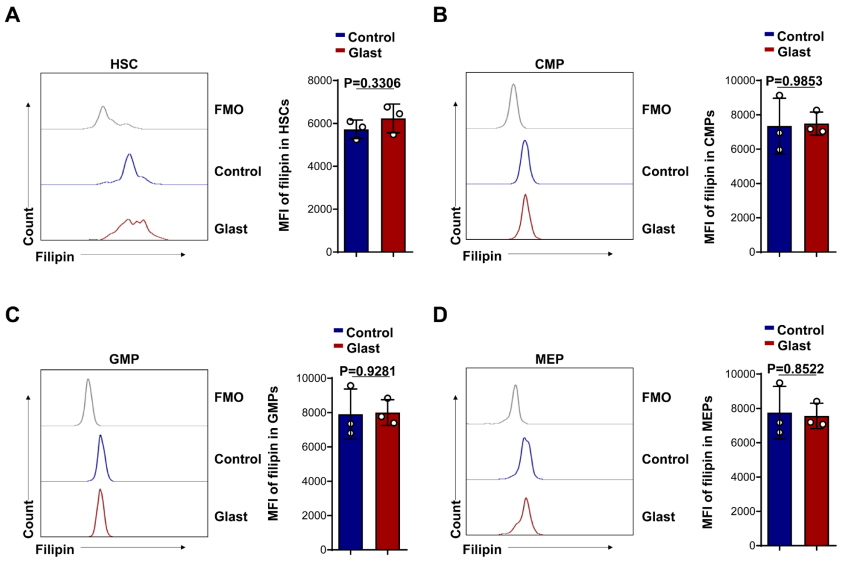

Supplementary Fig. S4: Cholesterol levels remain unchanged in HSCs and myeloid progenitors from Glast-CreERT;DTA mice.

A–D, Flow cytometric analysis of intracellular cholesterol levels using filipin staining in HSCs **(A)**, common myeloid progenitors (CMPs) **(B)**, granulocyte-monocyte progenitors (GMPs) **(C),** and megakaryocyte-erythroid progenitors (MEPs) **(D)** from Glast-CreERT;DTA and control mice ($n = 3$ per group). Mean fluorescence intensity (MFI) of filipin was comparable between groups across all cell types. FMO controls are shown for reference. Data are presented as mean ± s.d. *P* values were determined using two-tailed unpaired Student's *t*-tests. All experiments were independently repeated at least twice.

Supplementary Fig. S5

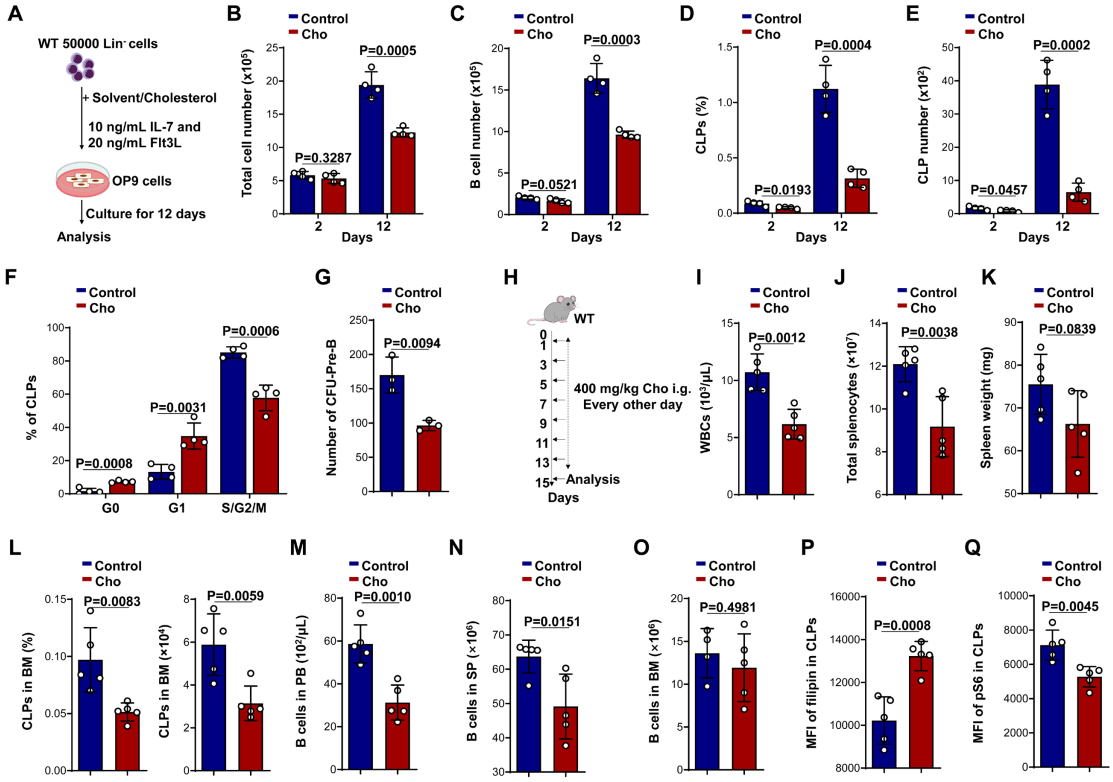

Supplementary Fig. S5: Cholesterol supplementation suppresses CLP expansion and B-cell differentiation *in vitro* and *in vivo*.

A, Experimental design of the *in vitro* B-cell differentiation assay, in which bone marrow (BM) Lin⁻ cells were cultured for 12 days on OP9 stromal cells with cholesterol (30 μg/mL) or vehicle supplemented with IL-7 and Flt3L. **B,** Total viable cell counts at days 2 and 12 ($n = 4$ per group). **C,** Absolute numbers of B220⁺ B cells were quantified by flow cytometry ($n = 4$ per group). **D-E,** Common lymphoid progenitor (CLP) frequencies **(D)** and absolute numbers **(E)** were assessed in cultured cells ($n = 4$ per group). **F,** CLP cell-cycle distribution on day 12 was analyzed by flow cytometry ($n = 4$ per group). **G,** Pre-B cell colony-forming potential was assessed by culturing BM cells in methylcellulose supplemented with cholesterol or vehicle under lymphoid-promoting conditions. Colonies were quantified on day 7 ($n = 3$ per group). **H,** Experimental scheme of *in vivo* cholesterol administration, in which wild-type mice received cholesterol (400 mg/kg) or vehicle by oral gavage every other day from day 1 to day 13, and were analyzed on day 15. **I-K**, Peripheral white blood cell (WBC) counts **(I)** ($n = 5$ per group), total splenocyte numbers **(J)** ($n = 5$

per group), and spleen weights **(K)** ($n = 5$ per group) at endpoint. **L,** CLP frequencies (left) and absolute numbers (right) in BM ($n = 5$ per group). **M-O,** Absolute numbers of $B220^+$ B cells in peripheral blood **(M)** ($n = 5$ per group), spleen **(N)** ($n = 5$ per group), and BM **(O)** ($n = 4$-5 per group). **P,** Intracellular cholesterol levels in sorted CLPs as assessed by filipin staining (mean fluorescence intensity, MFI) ($n = 5$ per group). **Q,** pS6 levels in CLPs, measured by flow cytometry ($n = 5$ per group). Data are presented as mean ± s.d. *P* values were calculated using two-tailed unpaired Student's *t*-tests. All experiments were independently repeated at least twice.

Supplementary Fig. S6

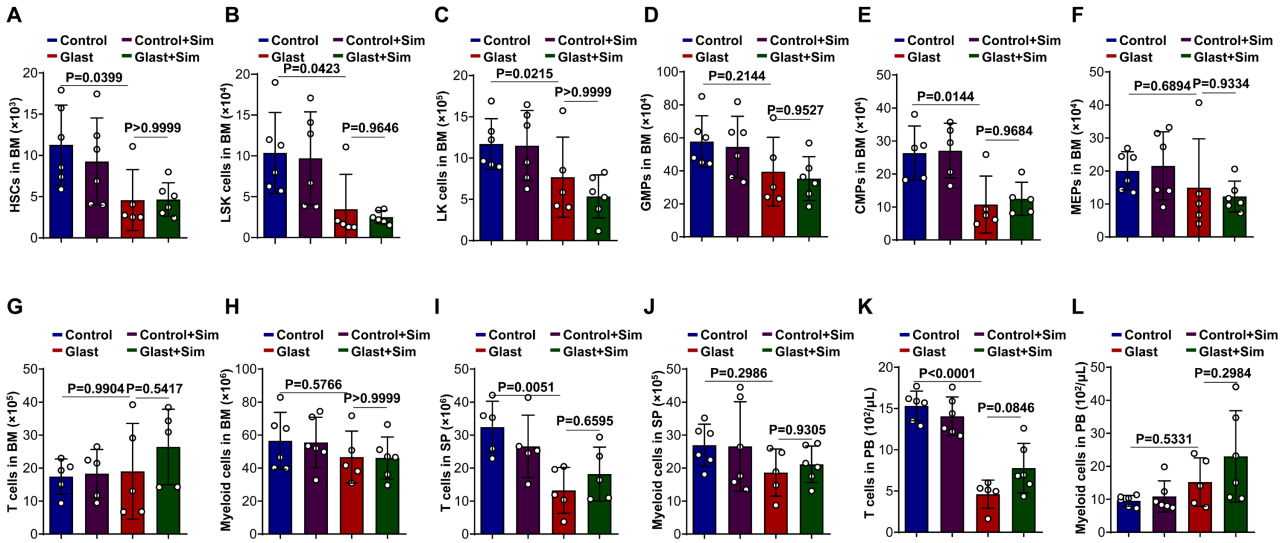

Supplementary Fig. S6: Intracerebroventricular simvastatin administration does not substantially alter non-lymphoid hematopoietic populations in Glast-CreERT;DTA mice. **A-F**, Absolute numbers of hematopoietic progenitors in bone marrow: HSCs **(A)**, LSK cells **(B)**, LK cells **(C)**, granulocyte-monocyte progenitors (GMPs) **(D)**, common myeloid progenitors (CMPs) **(E)**, and megakaryocyte-erythroid progenitors (MEPs) **(F)** in control, Glast-CreERT;DTA, and simvastatin-treated groups (*n* = 5-6 mice per group). **G-H,** Quantification of bone marrow T cells ($CD3^+$) **(G)** and myeloid cells ($CD11b^+Gr\text{-}1^+$) **(H)** in control, Glast-CreERT;DTA, and simvastatin-treated groups (*n* = 5-6 mice per group). **I, J,** Absolute numbers of T cells **(I)** and myeloid cells **(J)** in spleen (*n* = 5-6 mice per group). **K, L,** Absolute numbers of T cells **(K)** and myeloid cells **(L)** in peripheral blood (*n* = 5-6 mice per group). Data are presented as mean ± s. d. *P* values were determined by two-way ANOVA followed by Tukey's post hoc test. All experiments were independently repeated at least twice.

Supplementary Fig. S7

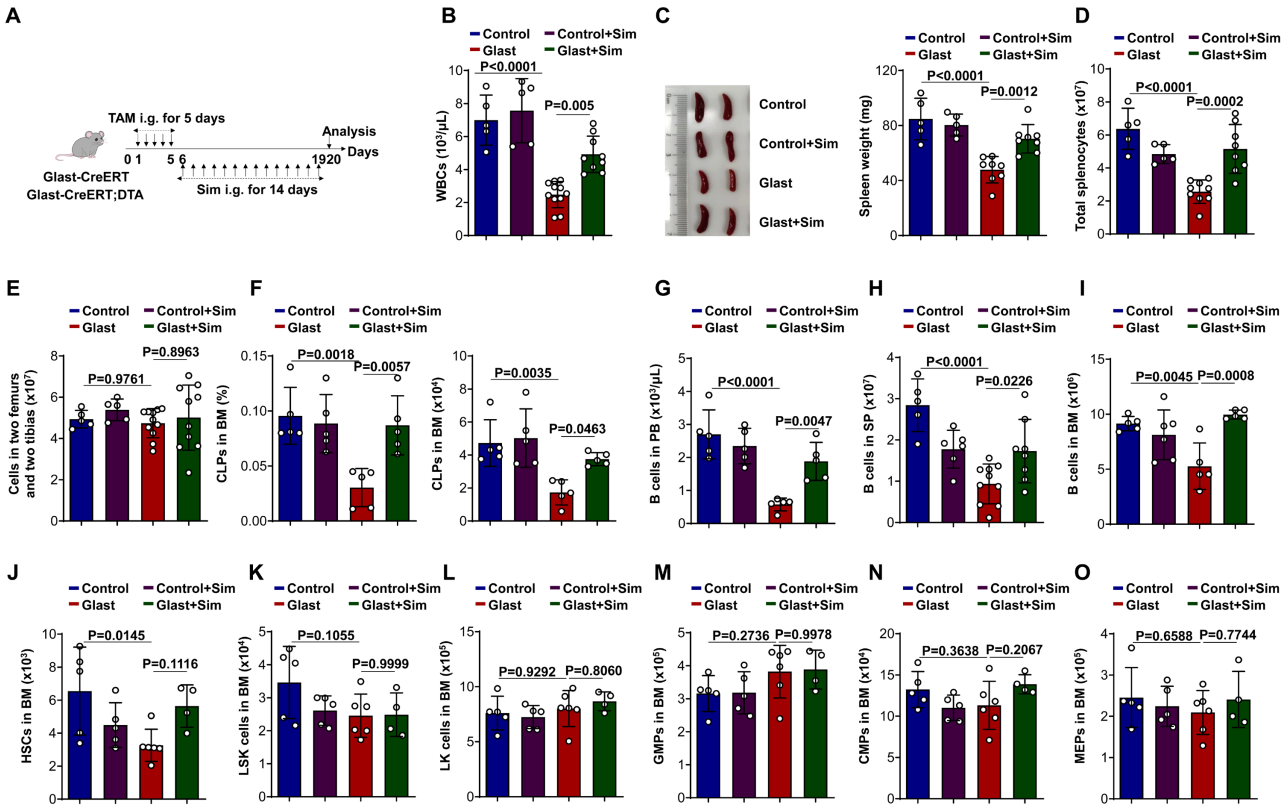

Supplementary Fig. S7: Oral simvastatin administration partially ameliorates lymphoid progenitor and B-cell defects in Glast-CreERT;DTA mice.

A, Experimental design: Glast-CreERT;DTA and control mice were treated with tamoxifen (TAM, oral gavage) once daily for 5 days to induce diphtheria toxin A (DTA) expression, followed by simvastatin (30 mg/kg per day, oral gavage) or vehicle administration for 14 days. Mice were analyzed on day 20. **B-E**, White blood cell (WBC) counts in peripheral blood **(B)**, representative spleen morphology **(C)**, spleen weights **(D)**, and total splenocyte counts **(E)** in control, Glast-CreERT;DTA, and simvastatin-treated groups (*n* = 5-11 mice per group). **F,** CLP frequencies (left) and absolute numbers (right) in bone marrow (*n* = 5 mice per group). **G-I,** Absolute numbers of B220⁺ B cellsin peripheral blood **(G)**, spleen **(H)**, and bone marrow **(I)** (*n* = 5-10 mice per group). **J-O,** Absolute numbers of HSCs **(J),** LSK cells **(K)**, LK cells **(L)**, granulocyte-monocyte progenitors (GMPs) **(M)**, common myeloid progenitors (CMPs) **(N)**, and megakaryocyte-erythroid progenitors (MEPs) **(O)** in bone marrow from control, Glast-CreERT;DTA, and simvastatin-treated mice (*n* = 4-6 mice per group). Data are presented as mean ± s.d. *P* values were

determined by two-way ANOVA followed by Tukey's post hoc test. All experiments were independently repeated at least twice.

Supplementary Fig. S8

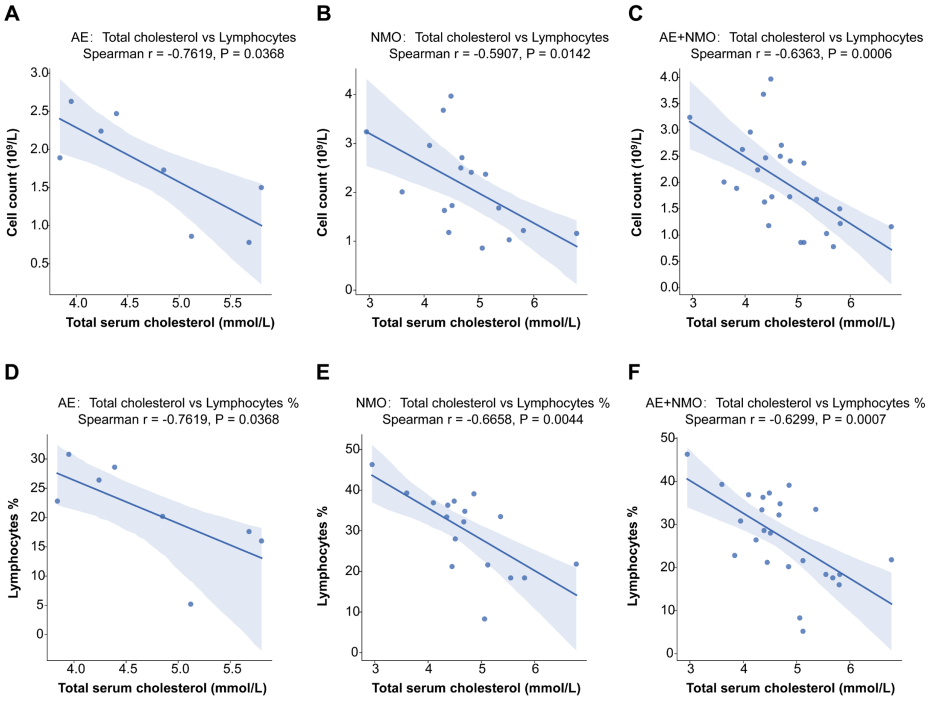

Supplementary Fig. S8: Serum cholesterol levels are inversely associated with periphery lymphocyte parameters in patients with neuroimmune disorders.

A-C, Spearman correlation between total serum cholesterol levels and absolute lymphocyte counts in patients with autoimmune encephalitis (AE) (**A**; *n* = 8), neuromyelitis optica (NMO) (**B**; *n* = 17), and the combined cohort (AE + NMO) (**C**; *n* = 25). **D-F,** Correlation between serum cholesterol levels and lymphocyte percentages among total white blood cells in AE (**D**; *n* = 8) NMO (**E**; *n* = 17), and the combined patients **(F**; *n* = 25). Each data point represents an individual patient. Spearman's correlation coefficient (*r*) and the two-tailed *P* value are indicated. Linear regression lines are shown with 95% confidence intervals (shaded areas).

Supplementary Fig. S9

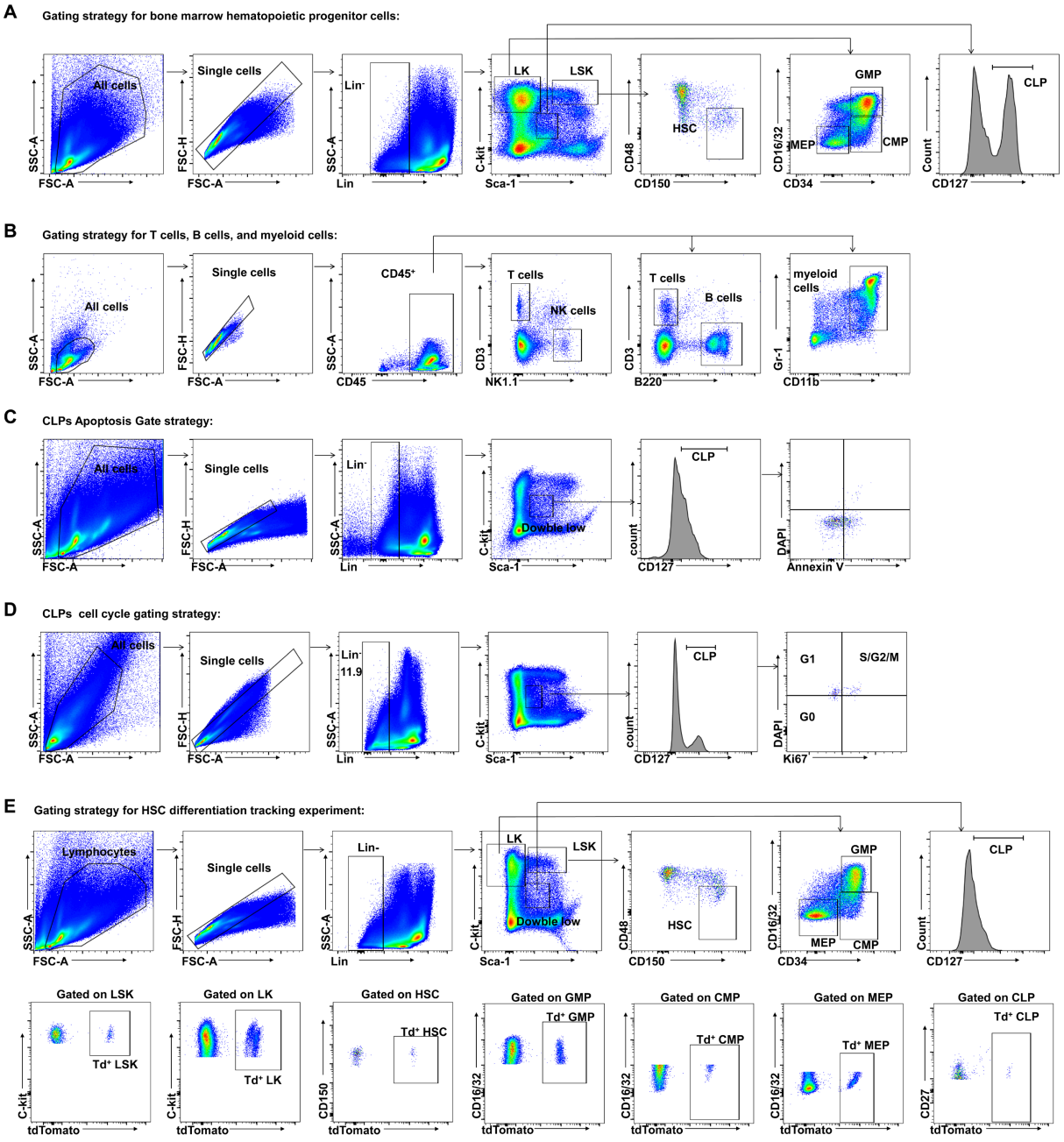

Supplementary Fig. S9: Gating strategies used in multiparameter fluorescence-activated cell sorting (FACS) analyses.

A, Gating strategy for the identification of hematopoietic stem cells (HSCs), LSK cells, and lineage-committed progenitors in bone marrow. Lineage-negative cells were defined using antibodies against CD3, Gr-1, CD11b, B220, and Ter-119. **B,** Gating strategy for T cells, B cells, and myeloid cells in bone marrow, spleen, and peripheral blood. **C,** Gating strategy for detecting apoptotic cells within the common lymphoid progenitor (CLP) population. **D,** Gating strategy for

CLP cell-cycle analysis based on DAPI staining. **E,** Gating strategy for HSC lineage tracing.

125 **Table S1. Clinical characteristics of samples from patients with neuroimmune disorders**

Sample ID	Age at Diagnosis	Gender	Diagnosis	Disease duration (Days)	Clinical status (relapse/remission)	Immunotherapy within 4 weeks	Comorbidities	Total serum cholesterol (mg/dL)	Total counts of lymphocytes (10^9/L)	Percentage of lymphocytes
1	26	Female	Neuromyelitis optica	6	Acute phase	No	None	2.95	3.24	46.3
2	39	Female	Neuromyelitis optica	60	Acute phase	No	None	5.12	2.37	21.6
3	63	Female	Neuromyelitis optica	30	Acute phase	No	None	4.86	2.41	39.1
4	56	Female	Neuromyelitis optica	30	Acute phase	No	None	3.6	2.01	39.3
5	21	Female	Neuromyelitis optica	30	Acute phase	No	Sjögren's syndrome	4.37	1.63	36.3
6	61	Female	Neuromyelitis optica	90	Acute phase	No	Hypertension	6.78	1.16	21.8
7	61	Female	Neuromyelitis optica	8	Acute phase	No	None	5.81	1.22	18.4
8	68	Male	Neuromyelitis optica	15	Acute phase	No	Hypertension	5.06	0.86	8.3
9	39	Female	Neuromyelitis optica	8	Acute phase	No	None	4.51	1.73	28
10	35	Female	Neuromyelitis optica	30	Acute phase	No	None	4.1	2.96	36.9
11	53	Female	Neuromyelitis optica	15	Acute phase	No	Hypertension/ Diabetes Mellitus	4.69	2.71	34.8
12	56	Female	Neuromyelitis optica	8	Acute phase	No	Hypertension/ Diabetes Mellitus	4.45	1.18	21.2

13	40	Female	Neuromyelitis optica	4	Acute phase	No	None	5.36	1.68	33.5
14	44	Female	Neuromyelitis optica	2	Acute phase	No	None	5.55	1.03	18.4
15	32	Female	Neuromyelitis optica	15	Acute phase	No	None	4.35	3.68	33.4
16	66	Female	Neuromyelitis optica	30	Acute phase	No	Diabetes Mellitus	4.49	3.97	37.3
17	27	Female	Neuromyelitis optica	60	Acute phase	No	None	4.67	2.5	32.2
18	27	Male	Autoimmune encephalitis	8	Acute phase	No	None	4.85	1.73	20.2
19	53	Female	Autoimmune encephalitis	10	Acute phase	No	None	5.12	0.86	5.2
20	52	Male	Autoimmune encephalitis	60	Acute phase	No	Diabetes Mellitus	4.39	2.47	28.6
21	50	Male	Autoimmune encephalitis	60	Acute phase	No	Hypertension	3.84	1.89	22.8
22	41	Female	Autoimmune encephalitis	18	Acute phase	No	None	5.68	0.78	17.6
23	67	Male	Autoimmune encephalitis	15	Acute phase	No	Hypertension/ Diabetes Mellitus	4.24	2.24	26.4
24	45	Female	Autoimmune encephalitis	90	Acute phase	No	None	3.95	2.63	30.8
25	75	Female	Autoimmune encephalitis	10	Acute phase	No	Hypertension/ Diabetes Mellitus	5.8	1.5	16.0